

Capacity and Delay of Unmanned Aerial Vehicle Networks with Mobility

Zhiqing Wei, Zhiyong Feng, Haibo Zhou, Li Wang, and Huici Wu

Abstract—Unmanned aerial vehicles (UAVs) are widely exploited in environment monitoring, search-and-rescue, etc. However, the mobility and short flight duration of UAVs bring challenges for UAV networking. In this paper, we study the UAV networks with n UAVs acting as aerial sensors. UAVs generally have short flight duration and need to frequently get energy replenishment from the control station. Hence the returning UAVs bring the data of the UAVs along the returning paths to the control station with a store-carry-and-forward (SCF) mode. A critical range for the distance between the UAV and the control station is discovered. Within the critical range, the per-node capacity of the SCF mode is $\Theta(\frac{n}{\log n})$ times higher than that of the multi-hop mode. However, the per-node capacity of the SCF mode outside the critical range decreases with the distance between the UAV and the control station. To eliminate the critical range, a mobility control scheme is proposed such that the capacity scaling laws of the SCF mode are the same for all UAVs, which improves the capacity performance of UAV networks. Moreover, the delay of the SCF mode is derived. The impact of the size of the entire region, the velocity of UAVs, the number of UAVs and the flight duration of UAVs on the delay of SCF mode is analyzed. This paper reveals that the mobility and short flight duration of UAVs have beneficial effects on the performance of UAV networks, which may motivate the study of SCF schemes for UAV networks.

Index Terms—Unmanned Aerial Vehicle; Scaling Laws; Store-Carry-and-Forward; Capacity; Delay

I. INTRODUCTION

UAVs are flexibly deployed in the challenging environment to accomplish tasks such as monitoring of air pollution or toxic gas leakage [1]. As shown in Fig. 1, UAVs act as aerial sensors to collect the data of air pollution and transmit data to the control station. Besides, UAVs can act as aerial base stations (BSs) to provide communication services to the areas with natural disasters, traffic congestions or concerts [2], [3]. UAVs can also act as aerial relays for vehicular networks to

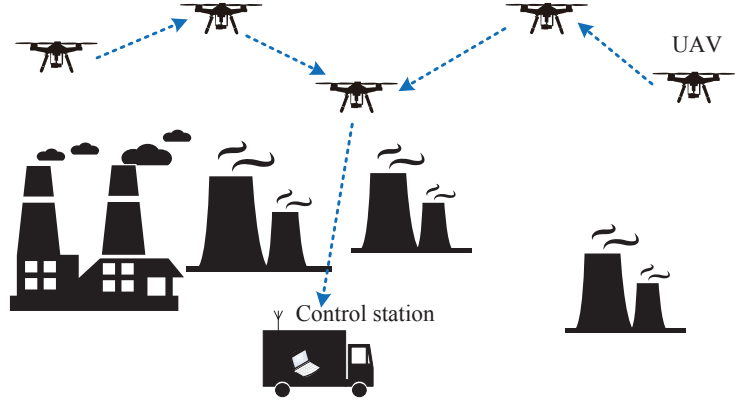


Fig. 1. The application scenario of UAVs.

improve the reliability of wireless links in vehicular networks [4]. Compared with single UAV system, the UAV swarm can complete missions in a more efficient and economical way [5], which makes UAV networking an emerging research field.

Generally, the studies of UAV networking mainly focus on the construction of broadband/robust UAV networks and the cooperation between UAV networks and other networks, such as vehicular networks, satellite networks, cellular networks. For the construction of broadband/robust UAV networks, Xiao *et al.* in [6] incorporated millimeter-wave into UAV networks to support high data rate transmission. Zhang *et al.* in [7] studied the spectrum sharing between UAV networks and ground cellular networks to improve the spectrum efficiency. Cai *et al.* in [8] and Jiang *et al.* in [9] designed the medium access control (MAC) protocol to construct robust UAV networks. Sbeiti *et al.* in [10] studied the routing protocols for airborne mesh networks. As to the cooperation between UAV networks and ground networks, Zhou *et al.* in [11] exploited multiple UAVs to act as aerial BSs to support vehicular networks. Sharma *et al.* in [12] adopted UAVs to enhance the coverage and capacity of two-tier cellular networks.

In UAV networks, the mobility of UAVs, the dynamic topology of UAV networks and the short flight duration will bring challenges for the design of network protocols and resource scheduling schemes. Facing these challenges, the literatures [6]-[12] studied the transmission schemes and protocols of UAVs. However, the mobility and fluid topology of UAVs have also beneficial effects on the UAV networks with appropriate network controlling and design. Mozaffari *et al.* in [13] studied the scenario that a single UAV acts as a flying BS for an underlaid ad hoc network, where the optimal altitude of UAV was derived to maximize the system sum-rate. They

This work is supported by the National Natural Science Foundation of China (No. 61631003, No. 61525101, No. 61601055).

Zhiqing Wei and Zhiyong Feng are with Key Laboratory of Universal Wireless Communications, Ministry of Education, School of Information and Communication Engineering, Beijing University of Posts and Telecommunications, Beijing, 100876, China (e-mail: {weizhiqing, fengzy}@bupt.edu.cn).

Haibo Zhou is with the School of Electronic Science and Engineering, Nanjing University, Nanjing 210023, China (e-mail: haibozhou@nju.edu.cn, h53zhou@uwaterloo.ca).

Li Wang is with Beijing Key Laboratory of Work Safety Intelligent Monitoring, School of Electronic Engineering, Beijing University of Posts and Telecommunications, Beijing, 100876, China. She is also with the Key Laboratory of the Universal Wireless Communications, Ministry of Education, China (e-mail: liwang@bupt.edu.cn).

Huici Wu is with the National Engineering Lab for Mobile Network Technologies, Beijing University of Posts and Telecommunications, Beijing 100876, China (e-mail: dailywu@bupt.edu.cn).

further optimized the density and altitude of multiple UAVs to maximize the coverage probability of ground networks [14]. Fadlullah *et al.* in [15] designed a trajectory control algorithm to improve end-to-end connectivity and delay of UAV assisted wireless networks. Besides acting as relays or BSs, UAVs can also act as mobile sinks to gather the data of sensor networks, where appropriate mobility control of UAVs can be designed to optimize the network performance. Ergezer *et al.* in [16] optimized the flight paths of UAVs to maximize the amount of collected data. Say *et al.* in [17] exploited the mobility information of UAV to assign different priorities to the nodes within UAV's coverage area to improve network capacity. Lyu *et al.* in [18] took advantage of the cyclical trajectory of fixed wing UAV to deliver the data of ground nodes.

The literatures [13]-[18] mainly focused on the mobility control algorithms to improve the performance of UAV-assisted networks. Actually, the intrinsic mobility pattern of UAVs can also be exploited to improve the performance of UAV networks. For example, the UAVs generally have short flight duration and they will frequently return to the control station to get energy replenishment, such as charging batteries. The returning UAVs can carry data for the UAVs along the returning paths to the control station with an SCF transmission manner. The network capacity can be boosted with SCF manner [19]. However, there are rare studies exploiting the intrinsic mobility pattern of UAVs to improve the performance of UAV networks.

In this paper, the mobility of UAVs is exploited to construct the SCF transmission manner. The scenario with UAVs acting as aerial sensors is considered, where the UAVs are uniformly distributed in a three-dimensional (3D) space or an aerial two-dimensional (2D) plane monitoring the environment. The returning UAVs are exploited to implement the SCF scheme. The capacity and delay scaling laws of UAV networks are studied. It is discovered that the capacity of SCF mode is $\Theta(\frac{n}{\log n})$ times higher compared with that of multi-hop mode. The delay of UAV networks with SCF mode is derived. The impact of the size of the entire region, the velocity of UAVs, the number of UAVs and the flight duration of UAVs on the delay of SCF mode is analyzed. Besides, the critical range is discovered. The capacity of the UAVs outside the critical range is smaller than that within the critical range, which results in the inhomogeneity of the capacity of UAV networks. The per-node capacity of UAV network with SCF mode is a piecewise function of the distance between the UAV and the control station with the critical as a threshold. Hence a mobility control scheme is proposed to eliminate the critical range such that the capacity scaling laws of all UAVs are the same. The mobility and the short flight duration are the features of UAVs. In common sense, the mobility and the short flight duration of UAVs bring challenges for the design of network protocols and resource scheduling schemes. However, the mobility and the short flight duration can also bring benefits for UAV networks. The SCF mode proposed in this paper turns the wasted returning time into treasure and makes the UAV networks scalable.

The remainder of this paper is organized as follows. The system model is introduced in Section II. In Section III and

TABLE I
KEY PARAMETERS AND NOTATIONS

Symbol	Description
n	Number of UAVs
v	Velocity of UAV
t_0	Flight duration of UAV
h	Altitude of UAVs in 2D UAV networks
W_1	Channel of multi-hop mode in 3D UAV networks
W_2	Channel of SCF mode in 3D UAV networks
W_1^*	Channel of multi-hop mode in 2D UAV networks
W_2^*	Channel from central cell to control station
W_3	Channel of SCF mode in 2D UAV networks
α	Path loss exponent
s_n	Side length of small cube in 3D UAV networks
ξ_n	Side length of small cell in 2D UAV networks
R_1	Per-hop capacity of 3D UAV networks
R_2	Per-hop capacity of 2D UAV networks
$\lambda_{SCF}(n)$	Per-node capacity of UAV networks with SCF mode
$f(n) = O(g(n))$	$\lim_{n \rightarrow \infty} \frac{f(n)}{g(n)} < \infty$
$f(n) = \Omega(g(n))$	$g(n) = O(f(n))$
$f(n) = \Theta(g(n))$	$f(n) = O(g(n))$ and $g(n) = O(f(n))$
$f(n) = o(g(n))$	$\lim_{n \rightarrow \infty} \frac{f(n)}{g(n)} = 0$
$f(n) = \omega(g(n))$	$g(n) = o(f(n))$
$f(n) \equiv g(n)$	This notation denotes $f(n) = \Theta(g(n))$
SCF	Store-carry-and-forward
PDF	Probability density function

Section IV, the capacity and delay scaling laws of 3D and 2D UAV networks are studied. In Section V, the main results are discussed. Finally, this paper is summarized in Section VI. The key parameters and notations are listed in Table I.

II. SYSTEM MODEL

The distribution of UAVs relies on the environment that UAVs are monitoring. For example, if UAVs are monitoring the air pollution, they will be distributed in 3D space. When the UAVs are monitoring the targets on ground, they may be distributed in 2D plane. In the literatures, the distribution of UAVs is various. For example, [14] assumes that the UAVs are distributed in 3D space. While [30] assumes that the UAVs are distributed in 2D plane. In order to study the capacity and delay of UAV networks comprehensively, 3D and 2D UAV networks, which are illustrated in Fig. 2(a) and Fig. 2(b), are considered in this paper.

A. Network Model

1) *3D UAV Networks*: In Fig. 2(a), n UAVs are uniformly distributed in a cube. The uniformly distributed UAVs can monitor the environment without priori information. A control station is placed at the center of the cube's bottom surface. The control station is "responsible for dispatching, coordinating, charging and collecting of UAVs" [19]. UAVs are regarded as sensors and the control station is the sink node collecting the data from all UAVs. When UAVs are about to exhaust energy, they will return to the control station to get energy replenishment. The returning UAVs are applied to implement the SCF scheme. As illustrated in Fig. 2(a), the returning UAV C can bring the data of UAV A to the control station.

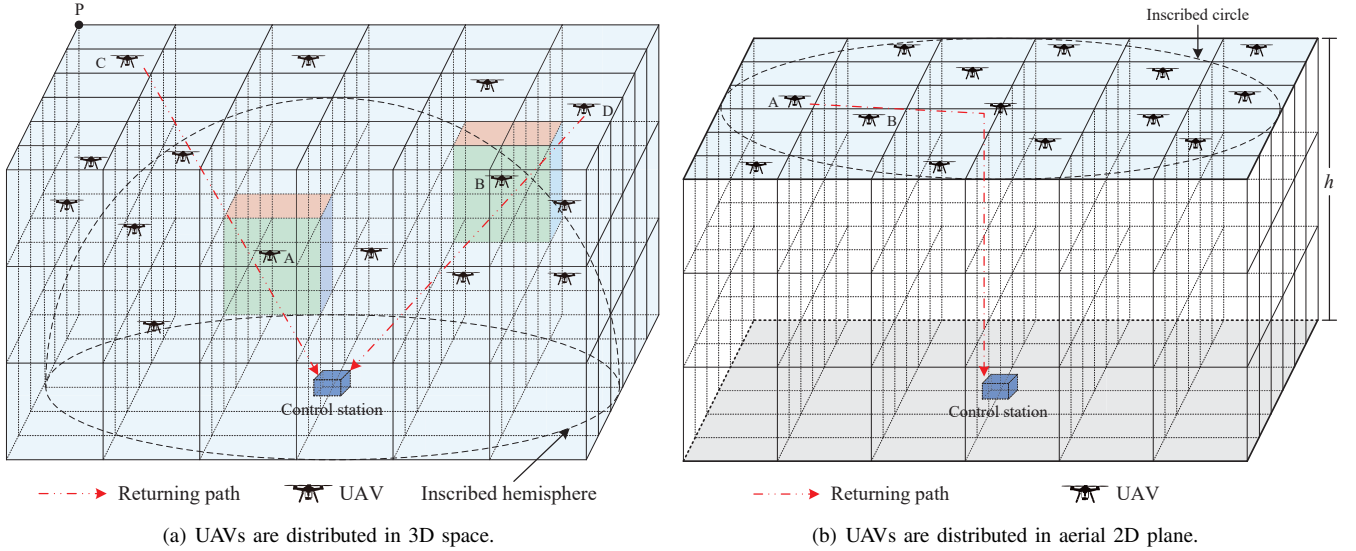


Fig. 2. Network model of UAV networks

The flight velocity and flight duration of UAV are defined as v and t_0 , respectively¹. The size of the cube is $2s \times 2s \times s$, where s satisfies the following inequality.

$$s < \frac{\sqrt{3} t_0 v}{3 \cdot 2}. \quad (1)$$

When $s = \frac{\sqrt{3} t_0 v}{3 \cdot 2}$, the distance between the vertex P in Fig. 2(a) and the control station is $\frac{t_0 v}{2}$, which is the maximum distance that a UAV can reach to guarantee that all UAVs can return within flight duration t_0 .

Then we consider the process of UAV dispatching. If UAVs are dispatched simultaneously at a moment, UAVs will return simultaneously to get energy replenishment, which brings heavy load to the control station. If the UAVs are sequentially dispatched, they will also return sequentially, which is beneficial for the control station. Thus each UAV is dispatched at a time instant uniformly distributed in the time interval $[0, t_0]$.

2) *2D UAV Networks*: Similar to [30], UAVs are flying at a given altitude. In Fig. 2(b), n UAVs are uniformly distributed on an aerial 2D square plane with side length $2s$ and altitude h . The control station is located on ground. The SCF mode can be applied when UAVs are distributed in an aerial 2D plane. As illustrated in Fig. 2(b), when a UAV returns to the control station, it firstly flies to the center of the plane. Then the returning UAV flies from the center of the plane to the control station. With this kind of returning path, the returning UAVs can be applied to implement the SCF scheme. As illustrated in Fig. 2(b), the returning UAV A can bring the data of UAV B to the control station. The relation between s and h is

$$\sqrt{2}s + h < \frac{t_0 v}{2}. \quad (2)$$

Sequential dispatching and returning is also consider in the 2D UAV networks to relieve the load of the control station.

¹The values of v and t_0 are assumed to be constant for simplicity. However, in practice, the values of v and t_0 are influenced by weather, wind, environment, flight attitude, etc. In this paper, we omit these factors to yields the capacity and delay scaling laws of UAV networks.

Hence each UAV is dispatched at a time instant uniformly distributed in the time interval $[0, t'_0]$ with $t'_0 = t_0 - \frac{2h}{v}$.

B. Network Protocols

1) *3D UAV Networks*: In 3D UAV networks, the multi-hop transmission mode and the SCF mode coexist to fully exploit transmission opportunities. The multi-hop transmission mode adopts straight-line routing [22], [32]. It is noted that straight-line routing is widely applied in scaling law analysis because it can provide analytical probabilistic model for the distribution of routings. There are two nonoverlapping wireless channels W_1 and W_2 for the multi-hop transmission mode and the SCF mode, respectively.

With the time division multiple access (TDMA) transmission scheme, the cube in Fig. 2(a) is split into small cubes. The side length of the small cubes is $s_n = (c_1 \frac{\log n}{n})^{1/3}$, where $c_1 = 4s^3 c_0$ with $c_0 > 0$. The small cubes are divided to organize the data transmissions. Only two UAVs in adjacent small cubes can transmit data to each other. With straight-line routing, the one hop transmission distance is $2\sqrt{3}s_n$, which means that a node can communicate with the nodes in the adjacent 26 cubes. With these configurations, we have the following lemma.

Lemma 1. ([19], [24]) *With n UAVs uniformly distributed in 3D space, the number of UAVs in a small cube with side length s_n is*

$$M = \Theta(\log n). \quad (3)$$

Proof: This lemma is the Lemma 1 in [19]. ■

According to Lemma 1, there exist UAVs in each small cube. Hence the connectivity of straight-line routing can be guaranteed. The 3D UAV networks adopt 27-TDMA scheme [19], [23]. As illustrated in Fig. 3, a cluster consists 27 small cubes. With the entire frame split into 27 time slots, the UAVs in each active cube share one time slot to transmit data. In addition, the cubes within one cluster take turns to be active

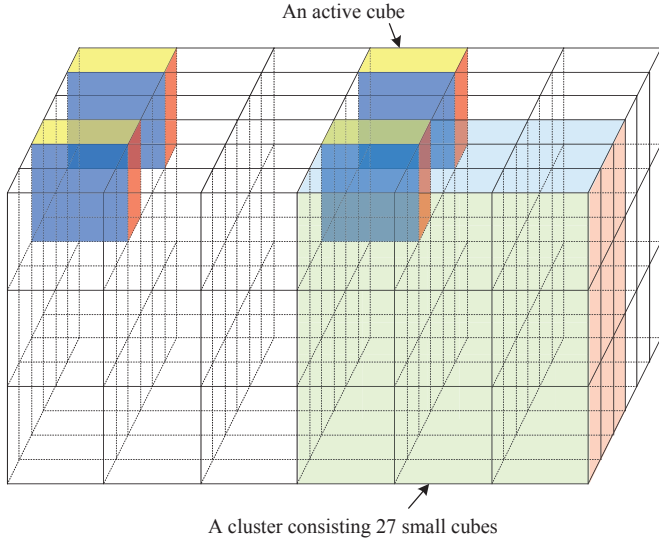


Fig. 3. 27-TDMA scheme.

in a round-robin manner. In such way, each UAV can take a time slot to transmit data. The transmit power is set as $P_0 s_n^\alpha$ to guarantee the transmission distance of $2\sqrt{3}s_n$, where α is the path loss exponent and P_0 is a constant. UAV A can transmit data to the UAVs in the adjacent 26 cubes. The neighborhood of UAV A is defined as the cluster consisting 27 cubes with UAV A in the central cube. If a returning UAV passes the neighborhood of UAV A, it can assist UAV A to deliver data to the control station. When multiple UAVs pass the neighborhood of UAV A simultaneously, only one returning UAV receives the data from UAV A.

2) *2D UAV Networks*: In 2D UAV networks, there are three nonoverlapping channels W_1^* , W_2^* and W_3^* . In multi-hop mode, data is transmitted to the central cell of the aerial 2D plane over channel W_1^* with straight-line routing [20], [22]. Then the central cell transmits the data to the control station over channel W_2^* . In SCF mode, data is transmitted over channel W_3^* . With the TDMA scheme, the entire square is split into small cells with side length $\xi_n = (c_3 \frac{\log n}{n})^{1/2}$, where $c_3 = 4s^2 c_2$ with $c_2 > 0$. Similar to Lemma 1, a small cell contains $\Theta(\log n)$ UAVs with high probability (*w.h.p.*).

There are UAVs in each small cell and the connectivity of straight-line routing is guaranteed. The transmit power is set as $P_1 \xi_n^\alpha$ to guarantee the transmit distance of $2\sqrt{2}\xi_n$, where P_1 is a constant. Hence a UAV can transmit data to another UAV in one of the adjacent 8 small cells. We define the cluster consisting the 9 cells with UAV B in the central cell as the neighborhood of UAV B. Then, if a returning UAV flies through the neighborhood of UAV B, it can assist UAV B to deliver data to the control station. The 2D UAV networks adopt the 9-TDMA scheme [22]².

C. Definitions

The per-node throughput and capacity of a UAV network are defined as follows.

²Letting $M = 3$ in Chapter 5 of [22], the multiple access scheme in [22] becomes 9-TDMA.

Definition 1. ([22][23]) *Per-node Throughput*: The per-node throughput of $\lambda(n)$ bits per second for a UAV network with n UAVs is feasible if there exists a scheduling scheme that every UAV can transmit data to the destination with data rate $\lambda(n)$.

The per-node throughput capacity of a UAV network is defined as follows.

Definition 2. ([22][23]) *Per-node Throughput Capacity*: The per-node throughput capacity for a UAV network with n UAVs is the order of $\Theta(f(n))$ bits per second if there are deterministic positive constants $c < c'$ such that

$$\lim_{n \rightarrow \infty} \Pr(\lambda(n) = cf(n) \text{ is feasible}) = 1, \quad (4)$$

while

$$\lim_{n \rightarrow \infty} \Pr(\lambda(n) = c'f(n) \text{ is feasible}) < 1. \quad (5)$$

Without causing confusion, the per-node throughput capacity is called per-node capacity for short in this paper.

III. SCALING LAWS: 3D UAV NETWORKS

A. The Capacity of UAV Networks with Multi-Hop Mode

With multi-hop mode, all UAVs transmit data to the control station. Hence the capacity of multi-hop mode is determined by the data rate of each UAV. The data rate of each node in 3D wireless ad hoc networks is as follows.

Lemma 2. ([19], [23]) *In 3D wireless ad hoc networks, the data rate of each node is*

$$R_1 \geq \begin{cases} \frac{1}{27} \Theta(n^{\frac{1}{3}(\alpha-3)}) & 2 < \alpha < 3 \\ \frac{1}{27} \Theta(\frac{1}{\log n}) & \alpha = 3 \\ \frac{1}{27} \Theta(1) & \alpha > 3 \end{cases}. \quad (6)$$

According to Lemma 2, the capacity of UAV networks with multi-hop mode is $\Theta(R_1)$.

B. The Capacity of UAV Networks with SCF Mode

In this section, the lower bound of the capacity of UAV networks with SCF mode is studied. An inscribed hemisphere with radius $L = s$ in Fig. 2(a) is adopted to estimate the lower bound of the number of returning UAVs. Similarly, a circumscribed hemisphere of the cube with radius $L = \sqrt{3}s$ can be used to derive the upper bound of the capacity of UAV networks with SCF mode.

In Fig. 4, when the UAVs in the shaded region of the spherical sector return, they will carry the data of UAV A to the control station. To simplify the analysis, the circumscribed sphere of the neighborhood of a UAV is adopted to replace the neighborhood of the UAV. Fig. 4 shows the circumscribed sphere of the neighborhood of UAV B. Denote x as the distance between the neighborhood of UAV A and the control station. Assuming k UAVs are contained in the shaded region of UAV A, k is a decreasing function with respect to x . The capacity of UAV networks with SCF mode is shown in the following theorem.

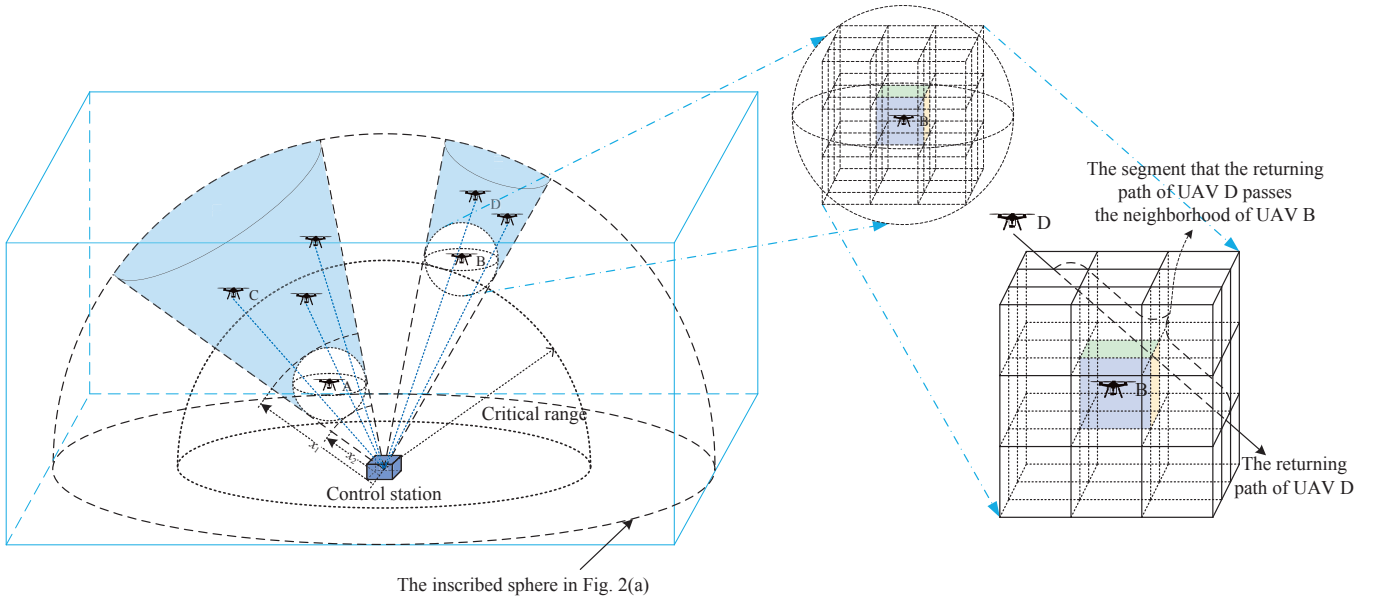


Fig. 4. UAV networks in 3D space.

Theorem 1. In 3D UAV networks, there exist x_1^* and x_2^* as follows.

$$x_1^* = \frac{1}{3} \frac{2^{1/3} L^6 u^2}{\left(27L^3 - 2L^9 u^3 + 3L^3 \sqrt{3(27 - 4L^6 u^3)}\right)^{1/3}} + \frac{1}{3} \frac{1}{2^{1/3}} \left(27L^3 - 2L^9 u^3 + 3L^3 \sqrt{3(27 - 4L^6 u^3)}\right)^{1/3} - \frac{1}{3} L^3 u = \Theta(1), \quad (7)$$

$$x_2^* = L - \Theta\left(\frac{1}{(\log n)^2}\right) + o\left(\frac{1}{(\log n)^3}\right), \quad (8)$$

where $u = \frac{16t_0 v}{9\pi c_1 c_4 \log n} \left(\log \frac{t_0 v}{c_1^{1/3} c_4} + \frac{1}{3} \log n - \frac{1}{3} \log \log n\right)$. x_1^* is defined as the critical range. When $x \leq x_1^*$, the order of the per-node capacity of 3D UAV networks with SCF mode is

$$\lambda_{SCF}(n) = \Theta\left(\frac{R_1}{\log n}\right) \quad (9)$$

w.h.p. When $x \geq x_2^*$, the order of the expectation of $\lambda_{SCF}(n)$ is

$$E[\lambda_{SCF}(n)] = \Theta\left(\frac{1 - \left(\frac{x}{L}\right)^3}{x^2} \frac{1}{t_0} R_1\right), \quad (10)$$

where $E[*]$ denotes the expectation of $*$.

Proof: The proof is provided in Appendix A. ■

Remark 1. The per-node capacity $\lambda_{SCF}(n)$ is a random variable because of the randomness of the network. We declare that $\lambda_{SCF}(n)$ is $\Theta\left(\frac{R_1}{\log n}\right)$ w.h.p. if $\lim_{n \rightarrow \infty} \Pr\left\{\lambda_{SCF}(n) = \Theta\left(\frac{R_1}{\log n}\right)\right\} = 1$, which is derived from Definition 2.

When $x \leq x_1^*$, the order of the per-node capacity of 3D UAV networks with SCF mode is (9), which is the data rate of each

node in Lemma 2 shared by the UAVs within a small cube. When $x \leq x_1^*$, there are multiple UAVs passing through the neighborhood of the UAV w.h.p. at any time. However, there is only one passing UAV communicating with the UAV. Hence the decrease of x within the critical range will not increase the per-node capacity of UAV network with SCF mode. When $x \leq x_1^*$, the per-node capacity of UAV network with SCF mode is $\lambda_{SCF}(n) = \Theta\left(\frac{R_1}{\log n}\right)$, which is highest. However, when $x > x_1^*$, the highest per-node capacity of $\Theta\left(\frac{R_1}{\log n}\right)$ can not be guaranteed. When $x \geq x_2^*$, since the time intervals that the returning UAVs flying through the neighborhood of a UAV are not overlapped, the per-node capacity of UAV network with SCF mode has clear form. Hence the $E[\lambda_{SCF}(n)]$ in this case is provided in (10). When $x_1 < x < x_2$, the form of the expectation of $E[\lambda_{SCF}(n)]$ is complex. The critical range x_1^* is a constant, which can not be eliminated via increasing the number of UAVs. Note that the $\lambda_{SCF}(n)$ within the critical range is maximum. The $\lambda_{SCF}(n)$ outside the critical range decreases with the increase of x .

The capacity of SCF mode for the UAVs outside the critical range is smaller than that within the critical range. Thus for the UAVs outside the critical range, the mobility of these UAVs needs to be controlled to improve the per-node capacity with SCF mode. In Section III-C, a mobility control scheme is designed for capacity improvement.

C. Flight Trajectories Control for Capacity Improvement

The per-node capacity of UAV networks with SCF mode relies on the distance between the UAV and the control station. When a UAV is outside of the critical range, the capacity with SCF mode is limited. Hence the flight trajectories of the UAVs outside the critical range can be controlled to improve the capacity with SCF mode. As illustrated in Fig. 5, when a UAV is about to return to the control station, firstly, the UAV flies upward with distance $J/2$. Secondly, the UAV flies

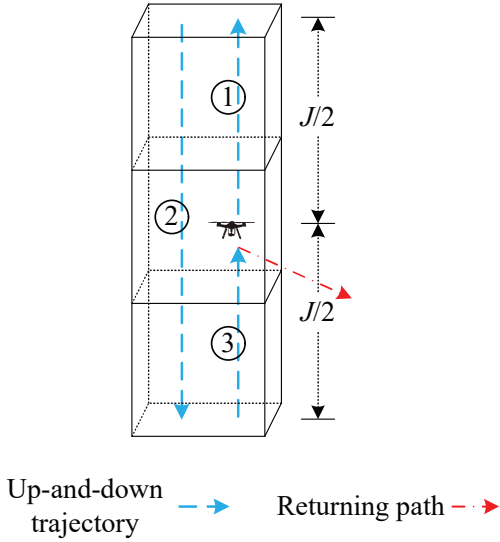


Fig. 5. The flight trajectory of a UAV with mobility control in 3D UAV networks.

downward with distance J . Thirdly, the UAV flies upward with distance $J/2$ and reaches the original spot. Finally, the UAV returns to the control station.

Notice that the flight trajectories denoted by the dotted lines in Fig. 5 are designed to collect the data of the UAVs along the flight trajectories, which are called “up-and-down trajectories”. With the “up-and-down trajectories”, a UAV outside of the critical range will encounter more UAVs passing through its neighborhood. Thus there are more transmission opportunities with mobility control, which will improve the capacity of UAV networks with SCF mode. The capacity with SCF mode for the UAVs outside the critical range is improved if J is a constant, as in the following theorem.

Theorem 2. *The UAVs outside the critical range fly following the up-and-down trajectories before they return. If J is a constant, the order of the per-node capacity of SCF mode for the UAVs outside the critical range is*

$$\lambda_{SCF}(n) = \Theta\left(\frac{R_1}{\log n}\right). \quad (11)$$

Proof: The proof is provided in Appendix B. ■

Remark 2. *According to Theorem 2, when J is a constant, all UAVs enjoy the same per-node capacity scaling laws of $\Theta\left(\frac{R_1}{\log n}\right)$ and the critical range is eliminated.*

Although the up-and-down trajectories improve the capacity of SCF mode, they reduce the time of environment monitoring for UAVs. Compared with the scheme without mobility control, the reduced time for environment monitoring is $\frac{2J}{v}$ per UAV.

D. Delay Analysis

The delay of SCF mode is studied in this section. The following theorem reveals the impact of the size of the entire region, the velocity of UAVs, the number of UAVs and the flight duration of UAVs on the delay of UAV networks.

Theorem 3. *The delay of UAV networks with SCF mode is*

$$D_{SCF}(n) \leq \frac{3L}{4v} + \Theta\left(t_0 \left(\frac{\log n}{n}\right)^{1/3}\right). \quad (12)$$

Proof: The proof is provided in Appendix C. ■

Remark 3. *The delay of SCF mode increases with the increase of t_0 , which is due to the fact that when t_0 is increased, the UAVs return infrequently such that the waiting time for a returning UAV is long. Moreover, with the increase of n , the waiting time for a returning UAV decreases, which will reduce the delay of SCF mode. According to (12), the delay of SCF mode is an increasing function of L and the delay of SCF mode is a decreasing function of v . The lower bound of $D_{SCF}(n)$ is $\frac{3L}{4v}$ since the term $\frac{3L}{4v}$ is the time that the returning UAV carries data to the control station.*

IV. SCALING LAWS: 2D UAV NETWORKS

A. The Capacity of UAV Networks with Multi-Hop Mode

In the multi-hop transmission, all the data will be sent to the central cell. Then the central cell sends data to the control station. The per-hop capacity of the 2D UAV networks is denoted as R_2 . And the capacity from the central cell to the control station is denoted as R_3 . The capacity of UAV networks is constraint by $\min\{R_2, R_3\}$. According to Lemma 6 in [27], R_2 is constant on the condition that the path loss exponent $\alpha > 2$, which is easy to be satisfied. Besides, R_3 is also constant because the central cell transmits data to the control station over a separated channel. The capacity of UAV networks with multi-hop transmission is

$$\Lambda_{MH} = \min\{R_2, R_3\}, \quad (13)$$

which is a constant.

B. The Capacity of UAV Networks with SCF Mode

The inscribed sphere with radius $K = s$ in Fig. 6 is adopted to estimate the lower bound of the number of returning UAVs to derive the lower bound of network capacity with SCF mode. In Fig. 6, when the UAVs in the shaded region return, the data of UAV B can be forwarded by them to the control station. Fig. 6 illustrates the circumscribed circle of the neighbourhood of a UAV. Define x as the distance between the circumscribed circle of UAV B’s neighborhood and the center of the plane. Define k as the number of UAVs in the shaded region. The capacity of SCF mode is revealed in the following theorem.

Theorem 4. *For 2D UAV networks, there exist x_1^* and x_2^* as follows.*

$$x_1^* = \frac{1}{2}\sqrt{4K^2 + u^2} - \frac{1}{2}u = \Theta(1), \quad (14)$$

$$x_2^* = K - \Theta\left(\frac{1}{(\log n)^2}\right), \quad (15)$$

where $u = \frac{8K^2 t_0 v}{3\sqrt{2}c_3 c_6 \log n} \left(\log \frac{t_0 v}{c_3^{1/2} c_6} + \frac{1}{2} \log n - \frac{1}{2} \log \log n\right)$. x_1^* is defined as critical range. When $x \leq x_1^*$, the order of the

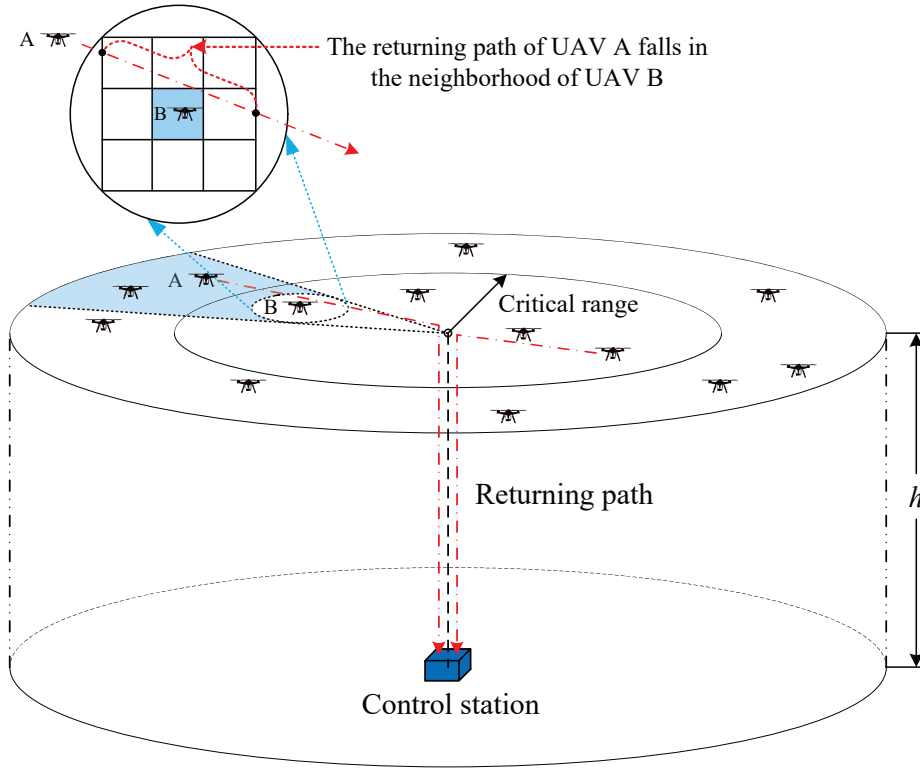


Fig. 6. UAV networks in 2D space.

per-node capacity of 2D UAV networks with SCF mode is

$$\lambda_{SCF}(n) = \Theta\left(\frac{R_2}{\log n}\right) \quad (16)$$

w.h.p. When $x \geq x_2^*$, the order of the expectation of $\lambda_{SCF}(n)$ is

$$E[\lambda_{SCF}(n)] = \Theta\left(\frac{\left(1 - \left(\frac{x}{K}\right)^2\right)}{x} \frac{1}{t_0} R_2\right). \quad (17)$$

Proof: The proof is provided in Appendix D. ■

Remark 4. The critical range for 2D UAV networks is a constant, which can not be eliminated via increasing the value of n . For the UAVs outside the critical range, $\lambda_{SCF}(n)$ still decreases with the increase of x .

For 2D UAV networks, similar mobility control scheme can be designed to eliminate the critical range and improve the capacity of UAV networks.

C. Flight Trajectories Control for Capacity Improvement

For 2D UAV networks, similar trajectories are designed for capacity improvement. As illustrated in Fig. 7, when a UAV is about to return, firstly, the UAV flies leftward with distance $J/2$. Secondly, the UAV flies rightward with distance J . Thirdly, the UAV flies leftward with distance $J/2$ and reaches the original spot. Finally, the UAV returns to the control station.

The flight trajectories denoted by the dotted lines in Fig. 7 are designed to collect the data of the UAVs along the flight trajectories, which are called “left-and-right trajectories”.

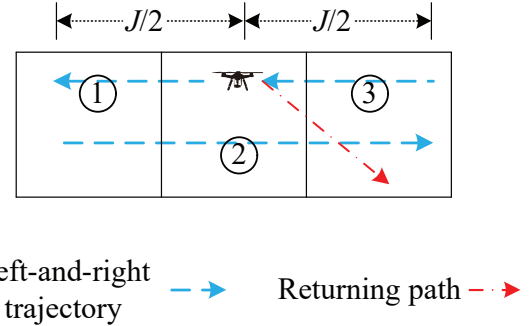


Fig. 7. The flight trajectory of a UAV with mobility control in 2D UAV networks.

With the left-and-right trajectories, Theorem 5 proves that the capacity of SCF mode for the UAVs outside the critical range can be improved if J is a constant.

Theorem 5. The UAVs outside the critical range fly following the left-and-right trajectories before they return. If J is a constant, the order of the per-node capacity of SCF mode for the UAVs that are outside the critical range is

$$\lambda_{SCF}(n) = \Theta\left(\frac{R_2}{\log n}\right). \quad (18)$$

Proof: The proof is provided in Appendix E. ■

Remark 5. With the control of flight trajectories, all UAVs can achieve the same per-node capacity of $\Theta\left(\frac{R_2}{\log n}\right)$, which means that the critical range is eliminated.

D. Delay Analysis

The delay of UAV networks with SCF mode is revealed in the following theorem.

Theorem 6. *The order of the delay of UAV networks with SCF mode is*

$$D_{SCF}(n) \leq \frac{2K}{3v} + \frac{h}{v} + \Theta\left(t_0 \left(\frac{\log n}{n}\right)^{1/2}\right). \quad (19)$$

Proof: The proof is provided in Appendix F. ■

Overall, the scaling laws for 3D and 2D UAV networks are analyzed. When the returning UAVs are exploited to implement the SCF scheme, the performance of UAV networks can be improved.

V. DISCUSSIONS

A. Per-node Capacity of UAV Networks with SCF Mode

The number of returning UAVs has an impact on the capacity of UAV networks with SCF mode. In Fig. 8(a), the control station is located in the origin and UAVs are distributed in 3D space. The number of potential returning UAVs at each location is denoted by color. The radius of the neighborhood of each UAV is $r = 0.8$. Note that the locations near the control station have a large number of returning UAVs. In Fig. 8(b), UAVs are distributed in the horizontal 2D plane. All UAVs fly to the origin and then fly to the control station. The radius of the neighborhood of each UAV is $r = 0.5$. Similar to 3D UAV networks, with the decrease of the distance between a UAV and the origin, the number of returning UAVs flying through the neighborhood of the UAV is increasing.

When the distance between a UAV and the control station x is smaller than the critical range x_1^* , $\lambda_{SCF}(n)$ is maximum. When $x \geq x_2^*$, the expectation of $\lambda_{SCF}(n)$ decreases with the increase of x . When $x \geq x_2^*$, the expectation of $\lambda_{SCF}(n)$ in 3D UAV networks is $\Theta\left(\frac{1 - (\frac{x}{L})^3}{x^2} \frac{1}{t_0} R_1\right)$. While the expectation of $\lambda_{SCF}(n)$ in 2D UAV networks is $\Theta\left(\frac{(1 - (\frac{x}{R})^2)}{x} \frac{1}{t_0} R_2\right)$. The function $g(x)$ is defined as follows.

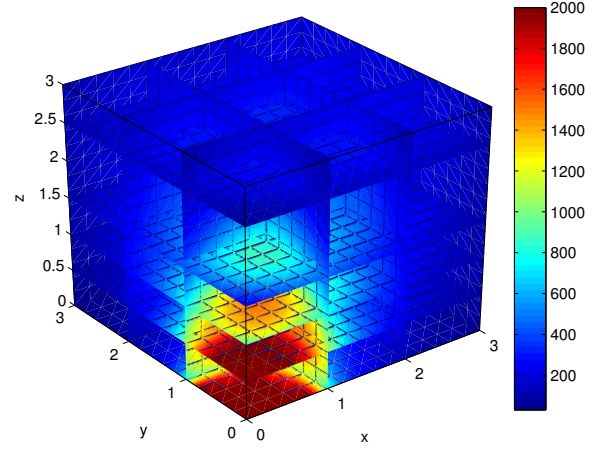
$$g(x) = \frac{\left(1 - \left(\frac{x}{K}\right)^2\right)}{x} - \frac{1 - \left(\frac{x}{L}\right)^3}{x^2}. \quad (20)$$

In this paper, we assume $K = L$. It can be proved that $g(x) \geq 0^3$. Hence with the increase of x , the capacity of UAV networks with SCF mode for 2D UAV networks decreases slower than that for 3D UAV networks.

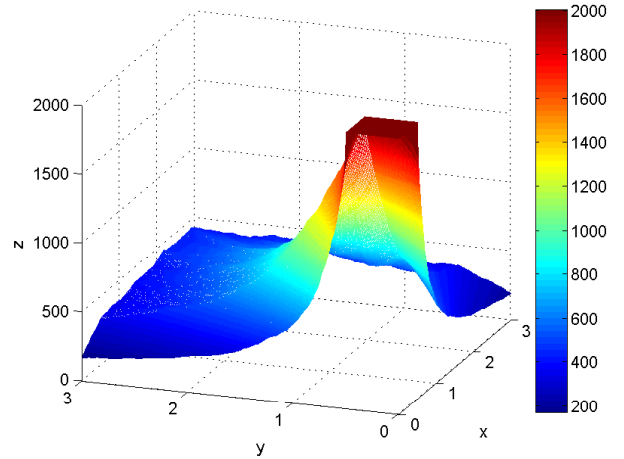
B. Impact of Flight Duration

The $\lambda_{SCF}(n)$ is a decreasing function of the flight duration t_0 , which is due to the fact that when t_0 increases, the number of returning UAVs decreases and $\lambda_{SCF}(n)$ decreases correspondingly. Besides, the critical range x_1^* decreases with the increase of t_0 , which will decrease the network capacity of UAV networks with SCF mode. Note that the delay is an increasing function of t_0 . According to Theorem 3 and Theorem 6, when t_0 increases, the waiting time for a returning UAV increases correspondingly, which will increase the delay.

³This conclusion can be proved by finding the derivative of $g(x)$.



(a) The number of returning UAVs in 3D space.



(b) The number of returning UAVs in 2D space.

Fig. 8. The number of returning UAVs.

C. Mobility Control

The mobility of UAVs can be controlled to eliminate the critical range and improve the network capacity with SCF mode. Note that when $J = \Theta(1)$, all UAVs can achieve the maximum capacity, namely, $\Theta\left(\frac{R_1}{\log n}\right)$ for 3D UAV networks and $\Theta\left(\frac{R_2}{\log n}\right)$ for 2D UAV networks. With mobility control, the capacity of 3D UAV networks with SCF mode is $\Theta\left(\frac{nR_1}{\log n}\right)$, which is $\Theta\left(\frac{n}{\log n}\right)$ times higher than that with multi-hop mode. Similarly, the capacity of 2D UAV networks with SCF mode is also $\Theta\left(\frac{n}{\log n}\right)$ times larger than that with multi-hop mode.

However, in the mobility control scheme, the UAVs switch to the returning state earlier than the schemes without mobility control. Hence the cost of mobility control scheme is that the time for environment monitoring is reduced. In this paper, the reduced time for environment monitoring is $\frac{2J}{v}$.

D. Delay of UAV Networks with SCF Mode

The delay of 3D UAV networks with SCF mode is illustrated in Fig. 9. Note that the delay tends to a constant when n

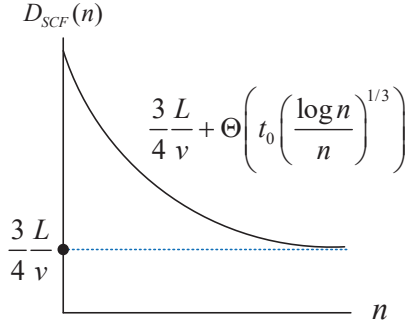


Fig. 9. The delay of 3D UAV networks with SCF mode.

tends to infinity, which means that the waiting time for a returning UAV tends to 0 when n tends to infinity. The waiting time for 3D and 2D UAV networks is upper bounded by $\Theta\left(t_0\left(\frac{\log n}{n}\right)^{1/3}\right)$ and $\Theta\left(t_0\left(\frac{\log n}{n}\right)^{1/2}\right)$ respectively. Notice that the waiting time for 3D UAV networks is larger than that for 2D UAV networks. The increase of t_0 will enlarge the waiting time and increase the delay of SCF mode. The time that a UAV flies to the control station is the lower bound of the delay of SCF mode.

VI. CONCLUSION

In this paper, the mobility and short flight duration of UAVs are exploited to improve the performance of UAV networks. With the observation that UAVs frequently return to the control station to get energy replenishment, we exploit the returning UAVs to implement SCF transmission scheme. Compared with the performance of multi-hop mode, The capacity of UAV networks with SCF mode improves $\Theta\left(\frac{n}{\log n}\right)$ times. However, a critical range is discovered, which is a watershed for the capacity of UAV networks. The per-node capacity of SCF mode for the UAVs outside the critical range is smaller than that within the critical range. Hence we propose a mobility control scheme to eliminate the critical range and improve the capacity of UAV networks. This paper has proved the advantages of SCF mode for UAV networks, which may motivate the design of more SCF transmission schemes for UAV networks.

ACKNOWLEDGMENTS

The authors appreciate editor and anonymous reviewers for their precious time and great effort in improving this paper.

APPENDIX A PROOF OF THEOREM 1

As illustrated in Fig. 4, a returning UAV flies through the neighborhood of a UAV with time $\frac{c_1^{1/3}c_4}{v}\left(\frac{\log n}{n}\right)^{1/3}$, where c_4 is a constant and $0 < c_4 \leq 3\sqrt{3}$. During the time that a returning UAV flies through the neighborhood of a cube, the amount of data carried by the returning UAV is $\frac{c_1^{1/3}c_4}{v}\left(\frac{\log n}{n}\right)^{1/3}R_1$.

Since sequential dispatching is considered, the k returning UAVs will return uniformly. We investigate the distribution of the time interval between two adjacent returning UAVs. According to order statistics [28], for an ascending sequence of uniformly distributed random variables Y_1, Y_2, \dots, Y_k , the PDF of $W_r = Y_{r+1} - Y_r$ is provided in Lemma 3. With some manipulations, the PDF of the time interval between two adjacent returning UAVs is

$$g(w) = \frac{k}{t_0} \left(1 - \frac{w}{t_0}\right)^{k-1}, \quad (21)$$

where k is a random variable following binomial distribution. According to Lemma 2 in [32], when n tends to infinity, the value of k has the same order with its expectation.

When the time interval $w \leq \frac{c_1^{1/3}c_4}{v}\left(\frac{\log n}{n}\right)^{1/3}$, multiple UAVs will pass through the neighborhood of UAV A and the UAVs in a small cube can share the following capacity with SCF mode.

$$\lambda_{SCF,cube}(n) = R_1. \quad (22)$$

Defining

$$k_{th} = \frac{t_0}{\frac{c_1^{1/3}c_4}{v}\left(\frac{\log n}{n}\right)^{1/3}}, \quad (23)$$

we will verify that if $k \geq k_{th} \log k_{th}$, (22) is established.

The probability that $w \leq \frac{c_1^{1/3}c_4}{v}\left(\frac{\log n}{n}\right)^{1/3}$ is

$$\begin{aligned} & \Pr \left\{ w \leq \frac{c_1^{1/3}c_4}{v}\left(\frac{\log n}{n}\right)^{1/3} \right\} \\ &= \int_0^{\frac{c_1^{1/3}c_4}{v}\left(\frac{\log n}{n}\right)^{1/3}} g(w)dw \\ &= 1 - \left(1 - \frac{1}{k_{th}}\right)^k. \end{aligned} \quad (24)$$

If $k \geq k_{th} \log k_{th}$, the limit of (24) with k_{th} tending to infinity is 1. Hence if $k \geq k_{th} \log k_{th}$, $\lambda_{SCF,cube}(n) = R_1$ *w.h.p.* Similarly, if $k \leq \frac{k_{th}}{\log k_{th}}$, the limit of (24) with k_{th} tending to infinity is 0. Hence if $k \leq \frac{k_{th}}{\log k_{th}}$, there is at most one UAV flying through the neighborhood of UAV A *w.h.p.* and the expectation of $\lambda_{SCF,cube}(n)$ in this case is

$$E[\lambda_{SCF,cube}(n)] = \frac{c_1^{1/3}c_4}{v}\left(\frac{\log n}{n}\right)^{1/3}R_1\frac{k}{t_0}. \quad (25)$$

In order to calculate the value of k , we derive the volume of the spherical sector in Fig. 4 as follows.

$$S_c = \frac{2\pi}{3}L^3 \left(1 - \frac{\sqrt{x^2 - r_n^2}}{x}\right), \quad (26)$$

where $r_n = \frac{3\sqrt{3}}{2}s_n$ is the radius of the circumscribed sphere of a UAV's neighborhood. In Fig. 4, the difference in the volume between the spherical sector with radius L and the spherical sector with radius x_2 is the upper bound of the volume of shaded region. Similarly, the difference in the volume between the spherical sector with radius L and the spherical sector with radius x_1 is the lower bound of the volume of shaded region.

With $x_1 = x + r_n$ and $x_2 = x - r_n$, the difference between x_1 and x_2 can be omitted in the asymptotic analysis because $\lim_{n \rightarrow \infty} r_n = 0$. Hence the volume of the shaded region is

$$\begin{aligned} S_u &= \frac{2\pi}{3} L^3 \left(1 - \frac{\sqrt{x^2 - r_n^2}}{x}\right) \left(1 - \left(\frac{x - r_n}{L}\right)^3\right) \\ &= \frac{2\pi}{3} L^3 \underbrace{\left(1 - \sqrt{1 - \left(\frac{r_n}{x}\right)^2}\right)}_{(a)} \left(1 - \frac{x^3}{L^3}\right). \end{aligned} \quad (27)$$

Notice that $\frac{r_n}{x}$ tends to 0. Using Taylor series expansion for the term (a) in (27), we have

$$S_u = \frac{2\pi}{3} L^3 \left(\frac{1}{2} \left(\frac{r_n}{x}\right)^2 + o\left(\left(\frac{r_n}{x}\right)^3\right)\right) \left(1 - \frac{x^3}{L^3}\right). \quad (28)$$

The shaded region of Fig. 4 averagely contains k_u UAVs.

$$k_u = n \frac{S_u}{4L^3} = \frac{\pi n}{6} \left(\frac{1}{2} \left(\frac{r_n}{x}\right)^2 + o\left(\left(\frac{r_n}{x}\right)^3\right)\right) \left(1 - \frac{x^3}{L^3}\right). \quad (29)$$

Letting $k_u \geq k_{th} \log k_{th}$, we have

$$\frac{1}{x^2} \left(1 - \frac{x^3}{L^3}\right) \geq u, \quad (30)$$

where

$$\begin{aligned} u &= \frac{16t_0v}{9\pi c_1 c_4 \log n} \left(\log \frac{t_0v}{c_1^{1/3} c_4} + \frac{1}{3} \log n - \frac{1}{3} \log \log n\right) \\ &= \Theta(1). \end{aligned} \quad (31)$$

(30) is equivalent to

$$\begin{aligned} x &\leq \frac{1}{3} \frac{2^{1/3} L^6 u^2}{\left(27L^3 - 2L^9 u^3 + 3L^3 \sqrt{3(27 - 4L^6 u^3)}\right)^{1/3}} \\ &+ \frac{1}{3} \frac{1}{2^{1/3}} \left(27L^3 - 2L^9 u^3 + 3L^3 \sqrt{3(27 - 4L^6 u^3)}\right)^{1/3} \\ &- \frac{1}{3} L^3 u \triangleq x_1^*. \end{aligned} \quad (32)$$

The x_1^* in (32) is defined as the critical range, which is a constant. Letting $k \leq \frac{k_{th}}{\log k_{th}}$, we have

$$\frac{1}{x^2} \left(1 - \frac{x^3}{L^3}\right) \leq \gamma, \quad (33)$$

where

$$\gamma = \frac{\frac{16t_0v}{9\pi c_1 c_4} \frac{1}{\log n}}{\log \frac{t_0v}{c_1^{1/3} c_4} + \frac{1}{3} \log n - \frac{1}{3} \log \log n} = \Theta\left(\frac{1}{(\log n)^2}\right). \quad (34)$$

Solving the inequality (33), the following relation can be derived.

$$x \geq L - \Theta\left(\frac{1}{(\log n)^2}\right) + o\left(\frac{1}{(\log n)^3}\right) \triangleq x_2^*. \quad (35)$$

The capacity of SCF mode for the UAVs in a small cube is summarized as follows.

$$\begin{aligned} \lambda_{SCF, cube}(n) &= R_1, & x &\leq x_1^*, \\ E[\lambda_{SCF, cube}(n)] &= \frac{c_1^{1/3} c_4}{v} \left(\frac{\log n}{n}\right)^{1/3} R_1 \frac{k}{t_0}, & x &> x_2^*. \end{aligned} \quad (36)$$

When $x > x_2^*$, we have

$$E[\lambda_{SCF, cube}(n)] = \Theta\left(\frac{1 - \left(\frac{x}{L}\right)^3}{x^2} \frac{\log n}{t_0} R_1\right) \leq R_1. \quad (37)$$

According to Lemma 1, $\lambda_{SCF, cube}(n)$ is shared by $\Theta(\log n)$ UAVs. Thus when $x \leq x_1^*$, the per-node capacity of UAV networks with SCF mode is $\lambda_{SCF}(n) = \Theta\left(\frac{R_1}{\log n}\right)$. When $x > x_2^*$, the expectation of $\lambda_{SCF}(n)$ is

$$E[\lambda_{SCF}(n)] = \frac{\Theta\left(\frac{1 - \left(\frac{x}{L}\right)^3}{x^2} \frac{\log n}{t_0} R_1\right)}{\Theta(\log n)} = \Theta\left(\frac{1 - \left(\frac{x}{L}\right)^3}{x^2} \frac{1}{t_0} R_1\right). \quad (38)$$

Lemma 3 ([28], [29]). *For an ascending sequence of random variables Y_1, Y_2, \dots, Y_k uniformly distributed in $[0, 1]$, the PDF of the range of Y_r and Y_{r+1} is*

$$f_{W_r}(w_r) = \frac{1}{B(1, k)} (1 - w_r)^{k-1}, \quad 0 \leq w_r \leq 1, \quad (39)$$

where

$$B(a, b) = \int_0^1 t^{a-1} (1-t)^{b-1} dt, \quad a > 0, b > 0. \quad (40)$$

APPENDIX B PROOF OF THEOREM 2

With mobility control, a UAV will encounter two kinds of passing UAVs, namely, the UAVs in up-and-down trajectories and the UAVs in returning paths. Theorem 1 studies the capacity of SCF mode contributed by the UAVs in returning paths. In this theorem, the capacity of SCF mode contributed by the UAVs in up-and-down trajectories is studied. As illustrated in Fig. 10, when the UAVs in the shaded cuboid fly following the up-and-down trajectories, they will pass through the neighborhood of UAV A. Hence with mobility control, the number of potential returning UAVs that fly through the neighborhood of UAV A in up-and-down trajectories is

$$N(J) = 9 \frac{\kappa J}{\left(c_1 \frac{\log n}{n}\right)^{1/3}} c_5 \log n, \quad (41)$$

where κ is a constant.

Define

$$k_{th} = \frac{t_0}{\frac{3c_1^{1/3}}{v} \left(\frac{\log n}{n}\right)^{1/3}}. \quad (42)$$

Similar to the proof of Theorem 1, if $N(J) \geq k_{th} \log k_{th}$, the amount of data that can be forwarded for the UAVs in a small cube by the UAVs in up-and-down trajectories per unit time is $\lambda'_{SCF, cube}(n) = R_1$ w.h.p. The value of $k_{th} \log k_{th}$ is

$$\begin{aligned} k_{th} \log k_{th} &= \frac{t_0v}{3c_1^{1/3}} \left(\frac{n}{\log n}\right)^{1/3} \times \\ &\left(\log \left(\frac{t_0v}{3c_1^{1/3}}\right) + \frac{1}{3} \log n - \frac{1}{3} \log \log n\right). \end{aligned} \quad (43)$$

Comparing (41) with (43), it can be proved that (41) and (43) have the same order. Thus if $J = \Theta(1)$, $\lambda'_{SCF, cube}(n) =$

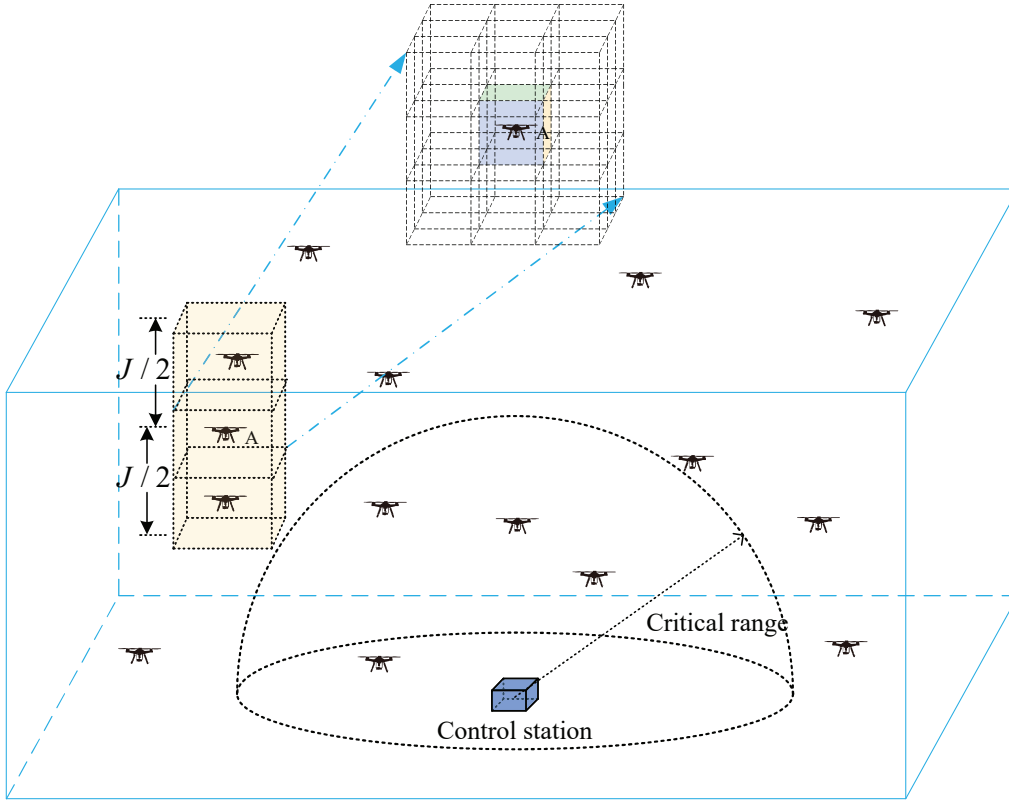


Fig. 10. The UAVs in the up-and-down trajectories.

R_1 . Note that the capacity of the UAVs in a small cube with SCF mode is the summation of the $\lambda'_{SCF,cube}(n)$ and the $\lambda_{SCF,cube}(n)$ in Theorem 1, which is shared by $\Theta(\log n)$ UAVs. Thus if $J = \Theta(1)$, the per-node capacity of UAV networks with SCF mode can be derived as (11).

APPENDIX C PROOF OF THEOREM 3

The delay of SCF mode consists the waiting time for a returning UAV and the time that the returning UAV carries data to the control station. Define the distance between a UAV and the control station as X , which is a random variable. The probability that a UAV falls in the spherical ring with inner radius x and outer radius $x + dx$ is as follows.

$$\begin{aligned} f(x)dx &= \Pr\{x \leq X \leq x + dx\} \\ &= \frac{\frac{2}{3}\pi(x+dx)^3 - \frac{2}{3}\pi(x)^3}{\frac{2}{3}\pi L^3} \\ &= \frac{(x+dx)^3 - (x)^3}{L^3} = \frac{3x^2 dx}{L^3}, \end{aligned} \quad (44)$$

where $f(x)$ is the probability density function (PDF) and the terms $o(dx)$ in (44) is omitted. Besides, for the UAV with distance x away from the control station, the delay to forward its data to the control station by a returning UAV is $\frac{x}{v}$.

Then we study the waiting time for a returning UAV, which is the time interval between two adjacent returning UAVs. As illustrated in Fig. 4, k UAVs are located in the shaded region of the UAV with distance x away from the control station, which will return sequentially within time t_0 . For the UAV

with distance x from the control station, the expectation of the delay with SCF mode is

$$\begin{aligned} D_{SCF}(n) &= \int_0^L f(x) \frac{x}{v} dx + \int_0^L f(x) \int_0^{t_0} wg(w) dw dx \\ &= \int_0^L \frac{3x^2}{L^3} \frac{x}{v} dx + \int_0^L \frac{3x^2}{L^3} \frac{t_0}{k+1} dx, \end{aligned} \quad (45)$$

where $g(w)$ is provided in (21). Replacing the k in (45) with the k_u in (29), we have

$$\begin{aligned} D_{SCF}(n) &= \int_0^L \frac{3x^2}{L^3} \frac{x}{v} dx + \int_0^L \frac{3x^2}{L^3} \frac{t_0}{k+1} dx \\ &= \frac{3}{4} \frac{L}{v} + \frac{36t_0}{\pi nr_n^2} \int_0^L \frac{x^4}{L^3 - (x - r_n)^3} dx. \end{aligned} \quad (46)$$

Since we have

$$\begin{aligned} &L^3 - (x - r_n)^3 \\ &= (L - x + r_n) \left(L^2 + (x - r_n)^2 + L(x - r_n) \right) \\ &\geq (L - x + r_n) L^2, \end{aligned} \quad (47)$$

the following inequality is established.

$$\begin{aligned} D_{SCF}(n) &\leq \frac{3}{4} \frac{L}{v} + \frac{36t_0}{\pi nr_n^2 L^2} \int_0^L \frac{x^4}{(L - x + r_n)} dx \\ &= \frac{3}{4} \frac{L}{v} + \frac{36t_0}{\pi nr_n^2 L^2} \times \\ &\quad \left(\frac{(L + r_n)^4 \log \frac{L+r_n}{r_n}}{-\frac{L}{12}(25L^3 + 52L^2 r_n + 42L r_n^2 + 12r_n^3)} \right) \\ &\triangleq D_{SCF,u}(n). \end{aligned} \quad (48)$$

With some manipulations, we have

$$\begin{aligned}
D_{SCF,u}(n) &\equiv \frac{3L}{4v} + \frac{36t_0}{\pi nr_n^2 L^2} \left(L \log \frac{L}{r_n} \right) \\
&= \frac{3L}{4v} + \frac{36t_0}{\pi nr_n^2 L} \left(\log \frac{2L}{3\sqrt{3}c_1^{1/3}} + \frac{1}{3} \log n - \frac{1}{3} \log \log n \right) \\
&\equiv \frac{3L}{4v} + \Theta \left(t_0 \left(\frac{\log n}{n} \right)^{1/3} \right).
\end{aligned} \tag{49}$$

This theorem is proved.

APPENDIX D

PROOF OF THEOREM 4

As illustrated in Fig. 6, a returning UAV flies through the neighborhood of UAV B with time $\frac{c_3^{1/2} c_6}{v} \left(\frac{\log n}{n} \right)^{1/2}$, where c_6 is a constant and $0 < c_6 \leq 3\sqrt{2}$. Defining

$$k_{th} = \frac{t'_0}{\frac{c_3^{1/2} c_6}{v} \left(\frac{\log n}{n} \right)^{1/2}}, \tag{50}$$

where $t'_0 = t_0 - \frac{2h}{v}$. Similar to the proof of Theorem 1, if $k \geq k_{th} \log k_{th}$, there is at least one returning UAV flying through the neighborhood of UAV B *w.h.p.* Then the UAVs in a small cube can share the following capacity with SCF mode.

$$\lambda_{SCF,cell}(n) = R_2. \tag{51}$$

If $k \leq \frac{k_{th}}{\log k_{th}}$, there is at most one returning UAV flying through the neighborhood of UAV B *w.h.p.* Therefore the expectation of the capacity for the UAVs in a small cell is

$$E[\lambda_{SCF,cell}(n)] = \frac{c_3^{1/2} c_6}{v} \left(\frac{\log n}{n} \right)^{1/2} R_2 \frac{k}{t'_0}. \tag{52}$$

In order to calculate the value of k , the area of the shaded region in Fig. 6 is derived. The area of the sector in Fig. 6 with radius K is

$$S_c = K^2 \arcsin \left(\frac{r_n}{x} \right), \tag{53}$$

where $r_n = \frac{3\sqrt{2}}{2} \xi_n$ is the radius of the circumscribed circle of UAV B's neighborhood. The difference of the area between the sector with radius K and the sector with radius $x + r_n$ is the lower bound of the area of shaded region. Similarly, the difference of the area between the sector with radius K and the sector with radius $x - r_n$ is the upper bound of the area of shaded region. Because $\lim_{n \rightarrow \infty} r_n = 0$, the term r_n can be omitted and we adopt the upper bound of the area of the shaded region as follows.

$$\begin{aligned}
S_u &= \left(K^2 - (x - r_n)^2 \right) \arcsin \left(\frac{r_n}{x} \right) \\
&\equiv \left(K^2 - x^2 \right) \arcsin \left(\frac{r_n}{x} \right).
\end{aligned} \tag{54}$$

The term $\frac{r_n}{x}$ tends to 0 when n tends to infinity. Using Taylor series expansion for the term $\arcsin \left(\frac{r_n}{x} \right)$, we have

$$S_u = \left(K^2 - x^2 \right) \left(\frac{r_n}{x} + o \left(\frac{r_n}{x} \right) \right). \tag{55}$$

The shaded region of Fig. 4 averagely contains k_u UAVs.

$$k_u = n \frac{S_u}{4K^2} = \frac{n}{4K^2} (K^2 - x^2) \left(\frac{r_n}{x} + o \left(\frac{r_n}{x} \right) \right). \tag{56}$$

Letting $k_u \geq k_{th} \log k_{th}$, we have

$$\frac{1}{x} (K^2 - x^2) \geq \frac{4K^2}{nr_n} k_{th} \log k_{th}. \tag{57}$$

Defining

$$u = \frac{4K^2}{nr_n} k_{th} \log k_{th} \tag{58}$$

and solving (57), we have

$$x \leq \frac{1}{2} \sqrt{4K^2 + u^2} - \frac{1}{2} u \triangleq x_1^*. \tag{59}$$

The x_1^* is defined as the critical range. It can be verified that $u = \Theta(1)$. Thus $x_1^* = \Theta(1)$. Letting $k \leq \frac{k_{th}}{\log k_{th}}$, we have

$$\frac{1}{x} (K^2 - x^2) \leq \gamma, \tag{60}$$

where

$$\gamma = \frac{\frac{8K^2}{3\sqrt{2}} \frac{t'_0 v}{c_3 c_6 \log n}}{\log \frac{t'_0 v}{c_3^{1/2} c_6} + \frac{1}{2} \log n - \frac{1}{2} \log \log n} = \Theta \left(\frac{1}{(\log n)^2} \right). \tag{61}$$

Solving the inequality (60), we have

$$x \geq K - \Theta \left(\frac{1}{(\log n)^2} \right) \triangleq x_2^*. \tag{62}$$

When $x > x_2^*$, we have

$$E[\lambda_{SCF,cell}(n)] = \frac{3\sqrt{2}c_3c_6}{8v} \frac{\left(1 - \left(\frac{x}{K}\right)^2\right) \log n}{x} \frac{1}{t_0} R_2 \leq R_2. \tag{63}$$

According to Lemma 1, $\lambda_{SCF,cell}(n)$ is shared by $\Theta(\log n)$ UAVs. When $x \leq x_1^*$, the per-node capacity of UAV networks with SCF mode is $\lambda_{SCF}(n) = \Theta \left(\frac{R_2}{\log n} \right)$. When $x > x_2^*$, the expectation of $\lambda_{SCF}(n)$ is

$$E[\lambda_{SCF}(n)] = \frac{\lambda_{SCF,cell}(n)}{\Theta(\log n)} = \Theta \left(\frac{\left(1 - \left(\frac{x}{K}\right)^2\right) \frac{1}{t'_0} R_2}{x} \right). \tag{64}$$

APPENDIX E

PROOF OF THEOREM 5

A UAV will encounter two kinds of passing UAVs with mobility control, namely, the UAVs in left-and-right trajectories and the UAVs in returning paths. The number of potential passing UAVs in left-and-right trajectories is

$$N(J) = 3 \frac{\kappa J}{\left(c_3 \frac{\log n}{n} \right)^{1/2}} c_9 \log n, \tag{65}$$

where κ is a constant and $c_9 \log n$ denotes the number of UAVs within a small cell. Define

$$k_{th} = \frac{t_0}{\frac{3c_3^{1/2}}{v} \left(\frac{\log n}{n} \right)^{1/2}}. \tag{66}$$

Similar to the proof of Theorem 2, it can be verified that $N(J) = k_{th} \log k_{th}$ if J is a constant. Thus Theorem 5 is proved.

APPENDIX F
PROOF OF THEOREM 6

Similar to the proof of Theorem 3, the delay of SCF mode consists the waiting time for a returning UAV and the time that the returning UAV carries data to the control station. Denote the distance between a UAV and the center of the plane as X . The probability that a UAV falls in the ring with inner radius x and outer radius $x + dx$ is

$$\begin{aligned} f(x)dx &= \Pr\{x \leq X \leq x + dx\} \\ &= \frac{\pi(x + dx)^2 - \pi x^2}{\pi K^2} = \frac{2x dx}{K^2}, \end{aligned} \quad (67)$$

where the terms $o(dx)$ is omitted in (67). The time that a UAV flies to the control station is $\frac{x}{v} + \frac{h}{v}$.

We investigate the waiting time for a returning UAV, which is the time interval between two adjacent returning UAVs. The shaded region in Fig. 6 contains k UAVs, which will return sequentially within time t_0 . The form of the PDF of the time interval between two adjacent returning UAVs is the same to (21), where the order of k is provided in (56). Thus for the UAV with distance x away from the center of the plane, the expectation of the delay is

$$\begin{aligned} D_{SCF}(n) &= \int_0^K f(x) \frac{x}{v} dx + \int_0^L f(x) \int_0^{t_0} wg(w) dw dx \\ &+ \frac{h}{v} = \int_0^K \frac{2x}{K^2} \frac{x}{v} dx + \int_0^K \frac{2x}{K^2} \frac{t_0}{k+1} dx + \frac{h}{v}. \end{aligned} \quad (68)$$

Substituting the k_u in (56) into the k in (68), we have

$$\begin{aligned} D_{SCF}(n) &= \int_0^K \frac{2x}{K^2} \frac{x}{v} dx + \frac{h}{v} \\ &+ \underbrace{\int_0^K \frac{2x}{K^2} \frac{t_0}{\frac{n}{4K^2} (K^2 - (x - r_n)^2) \frac{r_n}{x}} dx}_{(b)}, \end{aligned} \quad (69)$$

where the upper bound of the term (b) is

$$\begin{aligned} (b) &= \int_0^K \frac{2x}{K^2} \frac{t_0}{\frac{n}{4K^2} (K - x + r_n)(K + x - r_n) \frac{r_n}{x}} dx \\ &\leq \int_0^K \frac{2x}{K^2} \frac{t_0}{\frac{n}{4K^2} (K - x + r_n) K \frac{r_n}{x}} dx \\ &= \underbrace{\frac{8t_0}{nKr_n} \left((K + r_n)^2 \log \frac{K + r_n}{r_n} - \frac{K}{2} (3K + 2r_n) \right)}_{(c)}. \end{aligned} \quad (70)$$

With some manipulations similar to the derivation of (49), the term (c) is as follows.

$$(c) \equiv \Theta \left(t_0 \left(\frac{\log n}{n} \right)^{1/2} \right). \quad (71)$$

The delay of SCF mode is derived as (19).

REFERENCES

- [1] M. Rossi and D. Brunelli, "Autonomous Gas Detection and Mapping With Unmanned Aerial Vehicles," *IEEE Transactions on Instrumentation and Measurement*, vol. 65, no. 4, pp. 765-775, Apr. 2016.
- [2] M. Erdelj, E. Natalizio, K. R. Chowdhury, and I. F. Akyildiz, "Help from the Sky: Leveraging UAVs for Disaster Management," *IEEE Pervasive Computing*, vol. 16, no. 1, pp. 24-32, Jan. 2017.
- [3] I. Bor-Yaliniz and H. Yanikomeroglu, "The New Frontier in RAN Heterogeneity: Multi-Tier Drone-Cells," *IEEE Communications Magazine*, vol. 54, no. 11, pp. 48-55, Nov. 2016.
- [4] W. Shi, H. Zhou, J. Li, W. Xu, N. Zhang and X. Shen, "Drone Assisted Vehicular Networks: Architecture, Challenges and Opportunities," *IEEE Network*, vol. 32, no. 3, pp. 130-137, May/June. 2018.
- [5] L. Gupta, R. Jain, and G. Vaszkun, "Survey of Important Issues in UAV Communication Networks," *IEEE Communications Surveys & Tutorials*, vol. 18, no. 2, pp. 1123-1152, Secondquarter 2016.
- [6] Z. Xiao, P. Xia, and X.-G. Xia, "Enabling UAV Cellular with Millimeter-Wave Communication: Potentials and Approaches," *IEEE Communications Magazine*, vol. 54, no. 5, pp. 66-73, May 2016.
- [7] C. Zhang and W. Zhang, "Spectrum Sharing for Drone Networks," *IEEE Journal on Selected Areas in Communications*, vol. 35, no. 1, pp. 136-144, Jan. 2017.
- [8] Y. Cai, F. R. Yu, J. Li, Y. Zhou, and L. Lamont, "Medium Access Control for Unmanned Aerial Vehicle (UAV) Ad-Hoc Networks With Full-Duplex Radios and Multipacket Reception Capability," *IEEE Transactions on Vehicular Technology*, vol. 62, no. 1, pp. 390-394, Jan. 2013.
- [9] A. Jiang, Z. Mi, C. Dong, and H. Wang, "CF-MAC: A collision-free MAC protocol for UAVs Ad-Hoc networks," *IEEE Wireless Communications and Networking Conference (WCNC)*, pp. 1-6, Apr. 2016.
- [10] M. Sbeiti, N. Goddemeier, D. Behnke, and C. Wietfeld, "PASER: Secure and Efficient Routing Approach for Airborne Mesh Networks," *IEEE Transactions on Wireless Communications*, vol. 15, no. 3, pp. 1950-1964, Mar. 2016.
- [11] Y. Zhou, N. Cheng, N. Lu, and X. (Sherman) Shen, "Multi-UAV-Aided Networks: Aerial-Ground Cooperative Vehicular Networking Architecture," *IEEE Vehicular Technology Magazine*, vol. 10, no. 4, pp. 36-44, Dec. 2015.
- [12] V. Sharma, M. Bennis, and R. Kumar, "UAV-Assisted Heterogeneous Networks for Capacity Enhancement," *IEEE Communications Letters*, vol. 20, no. 6, pp. 1207-1210, Apr. 2016.
- [13] M. Mozaffari, W. Saad, M. Bennis, and M. Debbah, "Unmanned Aerial Vehicle with Underlaid Device-to-Device Communications: Performance and Tradeoffs," *IEEE Transactions on Wireless Communications*, vol. 15, no. 6, pp. 3949-3963, Jun. 2016.
- [14] M. Mozaffari, W. Saad, M. Bennis, and M. Debbah, "Efficient Deployment of Multiple Unmanned Aerial Vehicles for Optimal Wireless Coverage," *IEEE Communications Letters*, vol. 20, no. 8, pp. 1647-1650, Aug. 2016.
- [15] Z. M. Fadlullah, D. Takaishi, H. Nishiyama, N. Kato, and R. Miura, "A Dynamic Trajectory Control Algorithm for Improving the Communication Throughput and Delay in UAV-Aided Networks," *IEEE Network*, vol. 30, no. 1, pp. 100-105, Jan. 2016.
- [16] H. Ergezer and K. Leblebicioglu, "Path Planning for UAVs for Maximum Information Collection," *IEEE Transactions on Aerospace and Electronic Systems*, vol. 49, no. 1, pp. 502-520, Jan. 2013.
- [17] S. Say, H. Inata, J. Liu, and S. Shimamoto, "Priority-Based Data Gathering Framework in UAV-Assisted Wireless Sensor Networks," *IEEE Sensors Journal*, vol. 16, no. 14, pp. 5785-5794, Jul. 2016.
- [18] J. Lyu, Y. Zeng, and R. Zhang, "Cyclical Multiple Access in UAV-Aided Communications: A Throughput-Delay Tradeoff," *IEEE Wireless Communications Letters*, vol. 5, no. 6, pp. 600-603, Dec. 2016.
- [19] Z. Wei, H. Wu, S. Huang, and Z. Feng, "Scaling Laws of Unmanned Aerial Vehicle Network with Mobility Pattern Information," *IEEE Communications Letters*, vol. 21, no. 6, pp. 1389-1392, Jun. 2017.
- [20] P. Gupta and P. R. Kumar, "The capacity of wireless networks," *IEEE Transactions on Information Theory*, vol. 46, no. 2, pp. 388-404, Mar. 2000.
- [21] S. Hauert, S. Leven, J.-C. Zufferey, and D. Floreano, "Communication-based Swarming for Flying Robots," *International Workshop on Self-Organized System*, pp. 1-4, Dec. 2010.
- [22] X. Feng and P. R. Kumar, "Scaling laws for ad hoc wireless networks: An information theoretic approach," *Foundations and Trends in Networking*, vol. 1, no. 2, pp. 145-270, 2006.
- [23] P. Li, M. Pan, and Y. Fang, "Capacity bounds of three-dimensional wireless ad hoc networks," *IEEE/ACM Transactions on Networking*, vol. 20, no. 4, pp. 1304-1315, Aug. 2012.

- [24] Z. Wei, Z. Feng, X. Yuan, X. Feng, Q. Zhang, and X. Wang, "The Achievable Capacity Scaling Laws of 3D Cognitive Radio Networks," *IEEE International Conference on Communications (ICC)*, pp. 1-6, May 2016.
- [25] B. Liu, Z. Liu, and D. Towsley, "On the capacity of hybrid wireless networks," *IEEE International Conference on Computer Communications (INFOCOM)*, vol. 2, pp. 1543-1552, Mar.-Apr. 2003.
- [26] A. Zemlianov and G. Veciana, "Capacity of ad hoc wireless networks with infrastructure support," *IEEE Journal on Selected Areas in Communications*, vol. 23, no. 3, pp. 657-667, Mar. 2005.
- [27] C. Yin, L. Gao, and S. Cui, "Scaling Laws for Overlaid Wireless Networks: A Cognitive Radio Network versus a Primary Network," *IEEE/ACM Transactions on Networking*, vol. 18, no. 4, pp. 1317-1329, Aug. 2010.
- [28] H. A. David and H. N. Nagaraja, "Order Statistics," *Wiley*, 2003.
- [29] Z. Wei, Z. Feng, Q. Zhang, W. Li, and T. A. Gulliver, "The asymptotic throughput and connectivity of cognitive radio networks with directional transmission," *Journal of Communications and Networks*, vol. 16, no. 2, pp. 227-237, Apr. 2014.
- [30] J. Lyu, Y. Zeng, R. Zhang, and T. J. Lim, "Placement Optimization of UAV-Mounted Mobile Base Stations," *IEEE Communications Letters*, vol. 21, no. 3, pp. 604-607, Mar. 2017.
- [31] X. He, H. Zhang, T. Luo, W. Shi, "Network capacity analysis for cellular based cognitive radio VANET in urban grid scenario," *Journal of Communications and Information Networks*, vol. 2, no. 2, pp. 136-146, Jun. 2017.
- [32] Z. Wei, H. Wu, X. Yuan, S. Huang, and Z. Feng, "Achievable Capacity Scaling Laws of Three-Dimensional Wireless Social Networks," *IEEE Transactions on Vehicular Technology*, vol. 67, no. 3, pp. 2671-2685, Mar. 2018.
- [33] P. Gupta and P. R. Kumar, "Critical power for asymptotic connectivity," *37th IEEE Conference on Decision and Control*, vol. 1, pp. 1106-1110, Dec. 1998.
- [34] T. Zhang, S. Deng, H. Li, R. Hou, and H. Zhang, "A maximum flow algorithm for buffer-limited delay tolerant networks," *Journal of Communications and Information Networks*, vol. 2, no. 3, pp. 52-60, Sep. 2017.
- [35] Z. Guo, Z. Wei, Z. Feng, and N. Fan, "Coverage probability of multiple UAVs supported ground network," *Electronics Letters*, vol. 53, no. 13, pp. 885-887, Jun. 2017.